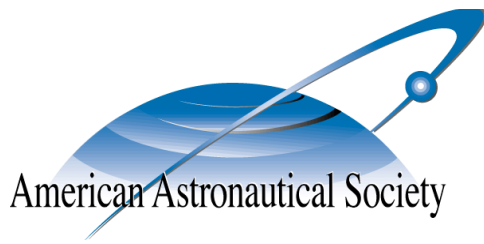


AAS 09-130



NONSINGULAR ATTITUDE FILTERING USING MODIFIED RODRIGUES PARAMETERS

Christopher D. Karlgaard* and Hanspeter Schaub†

AAS/AIAA Space Flight Mechanics

Savannah, Georgia

February 8-12, 2009

AAS Publications Office, P.O. Box 28130, San Diego, CA 92198

NONSINGULAR ATTITUDE FILTERING USING MODIFIED RODRIGUES PARAMETERS

Christopher D. Karlgaard[‡] and Hanspeter Schaub[§]

A method to estimate the general rigid body attitude using a minimal Modified Rodrigues Parameters (MRP) coordinate set is presented. The singularity avoidance technique is based on the stereographic projection properties of the MRP set, and makes use of a simple mapping relationship between MRP representations. Previous work has used the MRP duality to avoid singular attitude descriptions but has ignored the associated covariance transformation. This paper presents a mapping to transform the state covariance matrix between these two representations as the attitude description is mapped between the two possible MRP sets. Second-order covariance transformations suitable for divided difference filtering are also provided. The MRP filter formulation based on extended Kalman filtering and divided is compared with a standard multiplicative quaternion Kalman filter in an example problem.

INTRODUCTION

Attitude estimation techniques often make use of quaternions for the representing the attitude, for several reasons including globally nonsingular kinematics and linear state propagation.^{1,2} Techniques making use of quaternions as state variables are complicated by the quaternion constraint. The usual approach to satisfying the constraint is to estimate an error quaternion at each measurement update and then form the true quaternion estimate from the composition of the estimated error quaternion with the predicted quaternion based on the state transition matrix. Assuming small errors allows for the first three components of the quaternion to be estimated independently of the fourth component, which is essentially amounts to a linearization using small angle assumptions. Recently, constrained filtering approaches have been investigated by Zanetti and Bishop³ and Majji and Mortari.⁴ These approaches use a Lagrange multiplier formulation to solve a constrained filtering problem for all four components of the error quaternion, rather than using a linearization in order to enforce the quaternion norm constraint.

Other attitude parameterizations can be used, provided that a singularity avoidance method is employed to provide a valid attitude description at any condition. One representation with several attractive features are the Modified Rodrigues Parameters (MRP).⁵ The MRPs have several interesting properties. Firstly, the MRPs constitute a minimal three parameter set of variables that describe the orientation of a rigid body and are nonsingular for any rotation other than multiples of 2π . Tsiontras and Longuski⁶ discuss that the MRPs can be viewed as the result of a stereographic projection of the unit quaternion sphere onto a three-dimensional hyperplane. Schaub and Junkins⁷ use this insight to formulate a family of attitude coordinates called the Stereographic Orientation Parameters (SOP), which contain the MRPs as one particular solution of symmetric SOPs. As part of this

[‡]Senior Project Engineer, Analytical Mechanics Associates, Inc., 303 Butler Farm Road, Suite 104A, Hampton VA, 23666. karlgaard@ama-inc.com. Senior Member AIAA, Member AAS

[§]Associate Professor, Aerospace Engineering Sciences Department, University of Colorado, Boulder, CO, 80309-0431. hanspeter.schaub@colorado.edu. Associate Fellow AIAA, Member AAS

development it is noted that the MRPs are not unique, but rather there are always two possible MRP sets that can describe a particular orientation. This alternate MRP is known as the *shadow* MRP set. The shadow MRP set is singular for zero rotations, but is non-singular for rotations of 2π . This property allows for the development of a singularity avoidance method by switching to and from the shadow MRP set. For example, this switching procedure allows for non-singular optimal attitude control problems to be formulated using a minimal three-parameter family of MRPs as discussed in Ref. 8, in which an analytical mapping is developed for the MRP costates.

The application of MRPs to attitude estimation was first explored in Ref. 9 without discussion of singularity avoidance. Other examples make use of MRPs for representing attitude error rather than the global attitude, preferring to keep track of the quaternion.^{10,11} In these cases the MRP singularity is never encountered in practice but the additional computations to transform the MRP error estimate to the quaternion may not always be desirable. The two MRP sets are applied to attitude estimation problems as a singularity avoidance procedure in Refs. 12, 13, 14. In these cases, the transformation of the covariance matrix at the switching point has been ignored. The purpose of this paper is to introduce the covariance transformation to accompany the shadow MRP mapping for singularity avoidance in attitude estimation problems. The covariance transformation is introduced for Kalman filtering problems by using a first-order analytical mapping of the MRP and gyroscope bias state covariance to and from the shadow MRP set. Subsequently, a divided difference covariance transformation is introduced, suitable for the first and second-order divided difference filters introduced in Refs. 15 and 16. Numerical examples are provided that demonstrate the singularity avoidance technique applied to the spacecraft attitude estimation problem.

REVIEW OF MODIFIED RODRIGUES PARAMETER KINEMATICS

The MRPs are defined in terms of the quaternions (q_1, q_2, q_3, q_4) as

$$\boldsymbol{\sigma} = \frac{\mathbf{q}}{1 + q_4} = e \tan\left(\frac{\theta}{4}\right) \quad (1)$$

where $\mathbf{q} = (q_1, q_2, q_3)$ is the vector part of the quaternion, q_4 is the scalar part of the quaternion, e is the principal rotation axis, and θ is the principal rotation angle.

The shadow MRP set is defined as^{7,5}

$$\boldsymbol{\sigma}^S = -\frac{\boldsymbol{\sigma}}{\boldsymbol{\sigma}^T \boldsymbol{\sigma}} = e \tan\left(\frac{\theta - 2\pi}{4}\right) \quad (2)$$

Note that the MRP set $\boldsymbol{\sigma}$ behaves nearly linearly (with respect to θ) near the zero rotation and grows infinitely large after a revolution, while the shadow MRP set $\boldsymbol{\sigma}^S$ behaves linearly about 2π and is singular about the zero rotation. Further, while $\|\boldsymbol{\sigma}\| < 1$ (or > 1), $\boldsymbol{\sigma}$ describes the short (or long) rotation back to the origin, the shadow set $\boldsymbol{\sigma}^S$ describes the opposite rotation. The MRP and shadow MRP set can also be described as the *inner* and *outer* MRPs,¹⁷ respectively, where inner refers to the MRP set within the unit sphere ($\|\boldsymbol{\sigma}\| < 1$) and outer refers to the MRP set outside the unit sphere ($\|\boldsymbol{\sigma}\| > 1$). Both inner and outer sets lie on the unit sphere when $\|\boldsymbol{\sigma}\| = 1$.

As proposed in Ref. 7, the shadow MRP set can be exploited to yield a globally non-singular attitude description with a minimal three-parameter coordinate set at the expense of a discontinuity. To avoid the singularity, the MRP set is switched to the shadow set before reaching the singularity. A convenient switching condition is the unit magnitude surface $\|\boldsymbol{\sigma}\| = 1$, such that the composite

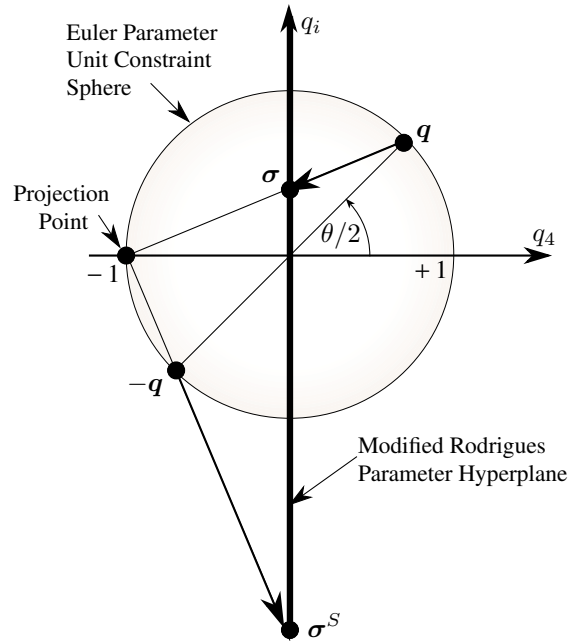


Figure 1. MRP Illustration as the Result of a Stereographic Projection

MRP description always satisfies $\|\sigma(t)\| \leq 1$. This surface represents all possible orientations where the body has performed a principal rotation relative to the origin of $\theta = \pi$. Note that on this surface there are two possible MRP sets that describe the same attitude.

Both sets of MRPs satisfy the same kinematic differential equation⁵

$$\dot{\sigma} = \frac{1}{4} \mathbf{B}(\sigma) \omega = \frac{1}{4} [(1 - \sigma^T \sigma) \mathbf{I} + 2\sigma^\times + 2\sigma\sigma^T] \omega \quad (3)$$

where ω is the angular velocity and σ^\times is the skew-symmetric cross product matrix.

Aside from providing a non-singular attitude description, another advantage of the combined MRP set restricted to $\|\sigma(t)\| \leq 1$ is that they behave nearly linearly for a large set of orientations. Figure 2 illustrates $\tan(\theta/4)$ and the linearized $\theta/4$ for rotations up to $\theta = \pi$.

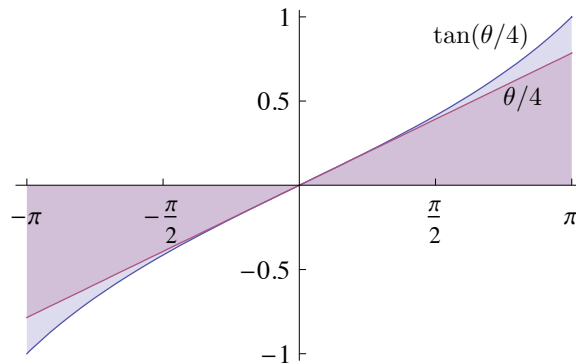


Figure 2. Illustration of the weakly nonlinear behavior of the MRPs restricted to $\|\sigma\| \leq 1$.

Having the analytical mapping between two possible MRP sets allows for two attitude motion descriptions to be solved simultaneously, using only one integration of the kinematic equations. After integrating the kinematic equations, the MRP set can be switched if $\|\sigma\| \geq 1$ and then the integration can continue. Note that the mapping in Eq. (2) is valid for any non-singular switching point. This observation allows the integration procedure to avoid the need to track the $\|\sigma\| = 1$ surface crossing precisely. Instead, the mapping step is performed only if the MRP set falls outside this surface.

Note that in general, the MRP can be switched to the shadow set at any surface of $\|\sigma\| \geq 1$. The shadow MRP mapping cannot be performed at conditions $\|\sigma\| < 1$. For example, suppose a switching condition of $\|\sigma\| = 1/2$ is specified. It follows from Eq. (2) that $\|\sigma^S\| = 2$. Since $2 > 1/2$, the MRP must immediately be switched back again and the cycle continues indefinitely. The most convenient switching condition is $\|\sigma\| \geq 1$ since that corresponds to the principal rotation angle of π . However there may be certain circumstances where other switching surfaces are favorable for a particular application. Therefore the covariance transformations developed in the following section are kept to the general case of any switching surface greater than one.

Note that it is possible to construct other minimal attitude coordinate sets which are even more linear with respect to the principal rotation angle θ than the MRPs. Reference 18 calls them the Higher Order Rodrigues Parameters (HORPs). Parameters τ can be developed which are written as

$$\tau = e \tan\left(\frac{\theta}{2N}\right) \quad (4)$$

where $N \geq 1$ is an integer value. These HORPs also contain multiple sets of possible values which can be used to avoid singular attitude descriptions. The MRP covariance mapping methods developed in this paper could be used for the HORB descriptions as well, but are not developed in this work.

ATTITUDE ESTIMATION USING MODIFIED RODRIGUES PARAMETERS

In order to use the MRP shadow set singularity avoidance technique for attitude estimation, a mapping must also be developed in order to transform the MRP state estimate error covariance matrix into the shadow set MRP state estimate error covariance matrix. In previous applications of the MRPs to attitude estimation problems, the state covariance matrix has implicitly been kept fixed during this switching to the shadow set.¹⁴ The following section describes the application of the shadow MRP set for singularity avoidance in the Kalman filter, including a first-order covariance transformation to accompany the MRP singularity avoidance mapping.

Kalman Filter Formulation

In typical attitude estimation problems, a gyroscope is used to sense the inertial angular velocity which is in turn used to integrate the kinematic equations of motion (3). A common approximation to the gyroscope dynamics is Farrenkopf's model,¹⁹ which considers the measured angular velocity to be of the form

$$\tilde{\omega} = \omega + \beta + \eta_\omega \quad (5)$$

$$\dot{\beta} = \eta_\beta \quad (6)$$

where $\tilde{\omega}$ is the sensed inertial angular velocity, ω is the true inertial angular velocity, β is the measurement bias, and η_ω and η_β are unbiased and uncorrelated random noise vectors. In this formulation, the state dynamics are expressed as

$$\dot{\mathbf{x}} = \mathbf{f}(\mathbf{x}, t) + \mathbf{g}(\mathbf{x}, \boldsymbol{\eta}, t) \quad (7)$$

where $\mathbf{x} = [\boldsymbol{\sigma}, \boldsymbol{\beta}]^T$, $\boldsymbol{\eta} = [\boldsymbol{\eta}_\omega, \boldsymbol{\eta}_\beta]^T$, and

$$\mathbf{f}(\mathbf{x}, t) = \begin{Bmatrix} (1/4) \mathbf{B}(\boldsymbol{\sigma}) (\tilde{\omega} - \boldsymbol{\beta}) \\ \mathbf{0} \end{Bmatrix} \quad (8)$$

$$\mathbf{g}(\mathbf{x}, \boldsymbol{\eta}, t) = \begin{Bmatrix} -(1/4) \mathbf{B}(\boldsymbol{\sigma}) \boldsymbol{\eta}_\omega \\ \boldsymbol{\eta}_\beta \end{Bmatrix} \quad (9)$$

It is assumed that a star tracker or some other generic attitude sensor is available to provide corrections to the attitude estimates formed by direct numerical integration of the angular velocity measurements, which are subject to error buildup due to integrating errors in the estimated bias and the random noise. The attitude sensing device is assumed to output an estimated MRP that relates the orientation of the body to the inertial frame. The estimates are assumed to be unbiased but with a superimposed random measurement noise. The output from such a sensor can be expressed as $\tilde{\boldsymbol{\sigma}} = \boldsymbol{\sigma} + \delta\boldsymbol{\sigma}$ where $\boldsymbol{\sigma}$ is the MRP representing the true orientation, $\tilde{\boldsymbol{\sigma}}$ is the ‘‘measured’’ MRP, and $\delta\boldsymbol{\sigma}$ is an error MRP with covariance matrix denoted by \mathbf{R} . For instance, the measured MRP could be an output from the algorithm described in Ref. 20, involving vector measurements. If discrete-time measurements of the MRP are available, then they can be incorporated into the state estimates using the extended Kalman filter, with state updates given by²¹

$$\hat{\mathbf{x}}_k = \bar{\mathbf{x}}_k + \mathbf{K}_k (\tilde{\boldsymbol{\sigma}} - \mathbf{H}_k \bar{\mathbf{x}}_k) \quad (10)$$

$$\hat{\mathbf{P}}_k = (\mathbf{I} - \mathbf{K}_k \mathbf{H}_k) \bar{\mathbf{P}}_k \quad (11)$$

where $\hat{\mathbf{x}}_k$ is the corrected state estimate after the measurement update at time t_k , $\hat{\mathbf{P}}_k$ is the corrected state covariance matrix, $\bar{\mathbf{x}}_k$ is the state prediction based on integration of the angular velocity measurements, $\bar{\mathbf{P}}_k$ is the predicted state covariance matrix, $\mathbf{H}_k = [\mathbf{I} \ \mathbf{0}]$, and \mathbf{K}_k is the Kalman gain matrix,

$$\mathbf{K}_k = \bar{\mathbf{P}}_k \mathbf{H}_k^T (\mathbf{H}_k \bar{\mathbf{P}}_k \mathbf{H}_k + \mathbf{R}_k) \quad (12)$$

The state predictions between MRP measurements can be determined by means of numerical integration of Eq. (7), or alternatively by means of analytical propagation using quaternion kinematics, as suggested in Ref. 12. The latter approach saves on the computation required of numerical integration by making use of the quaternion state transition matrix for propagating between the measurement points.

A first-order covariance prediction can be found by linearizing the Eq. (7), yielding

$$\delta\dot{\mathbf{x}} = \mathbf{F}\delta\mathbf{x} + \mathbf{G}\boldsymbol{\eta} \quad (13)$$

where

$$\mathbf{F} = \left. \frac{\partial \mathbf{f}}{\partial \mathbf{x}} \right|_{\mathbf{x}=\bar{\mathbf{x}}} = \begin{bmatrix} (1/2) [\bar{\boldsymbol{\sigma}} \bar{\boldsymbol{\omega}}^T - \bar{\boldsymbol{\omega}} \bar{\boldsymbol{\sigma}}^T - \bar{\boldsymbol{\omega}}^\times + \bar{\boldsymbol{\omega}}^T \bar{\boldsymbol{\sigma}} \mathbf{I}] & -(1/4) \mathbf{B}(\bar{\boldsymbol{\sigma}}) \\ \mathbf{0} & \mathbf{0} \end{bmatrix} \quad (14)$$

$$\mathbf{G} = \left. \frac{\partial \mathbf{g}}{\partial \boldsymbol{\eta}} \right|_{\mathbf{x}=\bar{\mathbf{x}}, \boldsymbol{\eta}=\mathbf{0}} = \begin{bmatrix} -(1/4) \mathbf{B}(\bar{\boldsymbol{\sigma}}) & \mathbf{0} \\ \mathbf{0} & \mathbf{I} \end{bmatrix} \quad (15)$$

where $\bar{\omega} = \tilde{\omega} - \bar{\beta}$, and $\delta \mathbf{x} = \mathbf{x} - \bar{\mathbf{x}}$.

The discrete-time covariance propagation between MRP measurements is

$$\bar{\mathbf{P}}_{k+1} = \Phi_k \bar{\mathbf{P}}_k \Phi_k^T + \tilde{\mathbf{Q}}_k \quad (16)$$

where Φ_k is the state transition matrix and $\tilde{\mathbf{Q}}_k$ is the process noise covariance matrix. Both of these quantities can be determined jointly through the relation^{21,22}

$$\exp \left(\begin{bmatrix} -\mathbf{F} & \mathbf{G}\mathbf{Q}\mathbf{G}^T \\ \mathbf{0} & \mathbf{F}^T \end{bmatrix} \delta t \right) = \begin{bmatrix} \mathbf{A}_{11} & \mathbf{A}_{12} \\ \mathbf{0} & \mathbf{A}_{22} \end{bmatrix} = \begin{bmatrix} \mathbf{A}_{11} & \Phi_k^{-1} \tilde{\mathbf{Q}}_k \\ \mathbf{0} & \Phi_k^T \end{bmatrix} \quad (17)$$

leading to the result $\Phi_k = \mathbf{A}_{22}^T$ and $\tilde{\mathbf{Q}}_k = \Phi_k \mathbf{A}_{12}$, where $\mathbf{Q} = \text{E} [\boldsymbol{\eta}\boldsymbol{\eta}^T]$ and $\delta t = t_{k+1} - t_k$.

During the course of state propagation or following the state update, the state can be switched to the shadow state if certain conditions are met, namely if $\|\boldsymbol{\sigma}\| > \sigma_r$ where σ_r is a threshold value. The shadow set transformation is given by $\mathbf{x}^S = \boldsymbol{\lambda}(\mathbf{x})$, where

$$\boldsymbol{\lambda}(\mathbf{x}) = \left\{ \begin{array}{c} -(\boldsymbol{\sigma}^T \boldsymbol{\sigma})^{-1} \boldsymbol{\sigma} \\ \boldsymbol{\beta} \end{array} \right\} \quad (18)$$

To examine the covariance transformation at the switching point, let the covariance matrix $\bar{\mathbf{P}}_k$ be decomposed into sub-matrices with the structure

$$\bar{\mathbf{P}}_k = \begin{bmatrix} \mathbf{P}_{\sigma\sigma} & \mathbf{P}_{\sigma\beta} \\ \mathbf{P}_{\sigma\beta}^T & \mathbf{P}_{\beta\beta} \end{bmatrix} \quad (19)$$

where $\mathbf{P}_{\sigma\sigma}$ is the covariance matrix of the MRP state, $\mathbf{P}_{\beta\beta}$ is the covariance matrix of the bias state, and $\mathbf{P}_{\sigma\beta}$ is the cross-correlation matrix between the MRP and the bias state. It follows that the covariance mapping to the shadow MRP set in the neighborhood of the reference MRP condition is given by

$$\begin{aligned} \bar{\mathbf{P}}_k^S &= \boldsymbol{\Lambda} \bar{\mathbf{P}}_k \boldsymbol{\Lambda}^T = \begin{bmatrix} \boldsymbol{\Lambda}_{11} & \mathbf{0} \\ \mathbf{0} & \mathbf{I} \end{bmatrix} \begin{bmatrix} \mathbf{P}_{\sigma\sigma} & \mathbf{P}_{\sigma\beta} \\ \mathbf{P}_{\sigma\beta}^T & \mathbf{P}_{\beta\beta} \end{bmatrix} \begin{bmatrix} \boldsymbol{\Lambda}_{11}^T & \mathbf{0} \\ \mathbf{0} & \mathbf{I} \end{bmatrix} \\ &= \begin{bmatrix} \boldsymbol{\Lambda}_{11} \mathbf{P}_{\sigma\sigma} \boldsymbol{\Lambda}_{11}^T & \boldsymbol{\Lambda}_{11} \mathbf{P}_{\sigma\beta} \\ \mathbf{P}_{\sigma\beta}^T \boldsymbol{\Lambda}_{11}^T & \mathbf{P}_{\beta\beta} \end{bmatrix} \end{aligned} \quad (20)$$

where

$$\boldsymbol{\Lambda} = \frac{\partial \boldsymbol{\lambda}}{\partial \mathbf{x}} = \begin{bmatrix} (2\sigma^{-4} \boldsymbol{\sigma} \boldsymbol{\sigma}^T - \sigma^{-2} \mathbf{I}) & \mathbf{0} \\ \mathbf{0} & \mathbf{I} \end{bmatrix} \quad (21)$$

and $\boldsymbol{\Lambda}_{11} = 2\sigma^{-4} \boldsymbol{\sigma} \boldsymbol{\sigma}^T - \sigma^{-2} \mathbf{I}$.

Note that this covariance mapping scales all MRP components. Assume that $\sigma = \|\boldsymbol{\sigma}\|$ is small, and the associated covariance components are small as well indicating good attitude knowledge. Then the corresponding shadow MRP set is stretched toward infinity due to σ being near zero. The associated covariance matrix for the shadow set is large as well, reflecting the large changes in coordinate values in the neighborhood of the singularity. The rate bias covariance is held constant during the MRP mapping, which is expected since the bias estimate itself is held constant in Eq. (18).

Divided Difference Filter Formulation

The Divided Difference Filter is one of several new estimation techniques that are collectively known as Sigma–Point Kalman Filters (SPKF). The divided difference filter arises from an alternate approach to the nonlinear state estimation and filtering problems than the EKF. Whereas the EKF is based on first–order Taylor series approximations, the divided difference filter relies on multidimensional interpolation formulas to approximate the nonlinear transformations. As a result of this approach, the filter does not require knowledge or existence of the partial derivatives of the system dynamics and measurement equations. In addition, it is straightforward to develop second–order filters by making use of higher–order interpolation formulas. SPKF–class filters have been applied to attitude estimation problems in Refs. 11, 14 and 23.

The First–Order (DD1) and Second–Order (DD2) Divided Difference Filters^{15,16} are reviewed in this section. The filter equations rely upon a discrete representation of the system dynamics, given by

$$\mathbf{x}_{k+1} = \boldsymbol{\phi}(\mathbf{x}_k, \boldsymbol{\eta}_k, t_k) \quad (22)$$

$$\boldsymbol{\sigma}_k = \mathbf{h}(\mathbf{x}_k, \delta\boldsymbol{\sigma}_k, t_k) \quad (23)$$

The following square-root decompositions of the covariance matrices are defined as

$$\hat{\mathbf{P}}_k = \hat{\mathbf{S}}_{x_k} \hat{\mathbf{S}}_{x_k}^T \quad (24)$$

$$\bar{\mathbf{P}}_k = \bar{\mathbf{S}}_{x_k} \bar{\mathbf{S}}_{x_k}^T \quad (25)$$

$$\mathbf{Q}_k = \mathbf{S}_{\eta_k} \mathbf{S}_{\eta_k}^T \quad (26)$$

$$\mathbf{R}_k = \mathbf{S}_{\delta\sigma_k} \mathbf{S}_{\delta\sigma_k}^T \quad (27)$$

Also, the j th column of $\bar{\mathbf{s}}_{x_k}$ is referred to as $\bar{\mathbf{s}}_{x_{k_j}}$; likewise for the other matrices.

First–Order Divided Difference Filter The DD1 filter makes use of first–order divided differences to approximate the system and measurement dynamics rather than the first–order Taylor series expansions used in the EKF. The following matrices of first–order divided differences are defined as

$$\mathbf{S}'_{x\hat{x}_{k_i,j}} = \frac{1}{2c} [\boldsymbol{\phi}_i(\hat{\mathbf{x}} + c\hat{\mathbf{s}}_{x_j}, \bar{\boldsymbol{\eta}}_k, t_k) - \boldsymbol{\phi}_i(\hat{\mathbf{x}}_k - c\hat{\mathbf{s}}_{x_j}, \bar{\boldsymbol{\eta}}_k, t_k)] \quad (28)$$

$$\mathbf{S}'_{x\eta_{k_i,j}} = \frac{1}{2c} [\boldsymbol{\phi}_i(\hat{\mathbf{x}}_k, \bar{\boldsymbol{\eta}}_k + c\mathbf{s}_{\eta_j}, t_k) - \boldsymbol{\phi}_i(\hat{\mathbf{x}}_k, \bar{\boldsymbol{\eta}}_k - c\mathbf{s}_{\eta_j}, t_k)] \quad (29)$$

$$\mathbf{S}'_{\sigma\bar{x}_{k_i,j}} = \frac{1}{2c} [\mathbf{h}_i(\bar{\mathbf{x}}_k + c\bar{\mathbf{s}}_{x_j}, \delta\bar{\boldsymbol{\sigma}}_k, t_k) - \mathbf{h}_i(\bar{\mathbf{x}}_k - c\bar{\mathbf{s}}_{x_j}, \delta\bar{\boldsymbol{\sigma}}_k, t_k)] \quad (30)$$

$$\mathbf{S}'_{\sigma\delta\sigma_{k_i,j}} = \frac{1}{2c} [\mathbf{h}_i(\bar{\mathbf{x}}_k, \delta\bar{\boldsymbol{\sigma}}_k + c\mathbf{s}_{\delta\sigma_j}, t_k) - \mathbf{h}_i(\bar{\mathbf{x}}_k, \delta\bar{\boldsymbol{\sigma}}_k - c\mathbf{s}_{\delta\sigma_j}, t_k)] \quad (31)$$

where c is the divided–difference perturbing parameter.

The state, state root–covariance, measurement, and measurement root-covariance predictions are given by

$$\bar{\mathbf{x}}_{k+1} = \boldsymbol{\phi}(\hat{\mathbf{x}}_k, \bar{\boldsymbol{\eta}}_k, t_k) \quad (32)$$

$$\bar{\mathbf{S}}_{x_{k+1}} = \mathcal{H}([\mathbf{S}'_{x\hat{x}_k} \quad \mathbf{S}'_{x\eta_k}]) \quad (33)$$

$$\bar{\boldsymbol{\sigma}}_k = \mathbf{h}(\bar{\mathbf{x}}_k, \delta\bar{\boldsymbol{\sigma}}_k, t_k) \quad (34)$$

$$\mathbf{S}_{\sigma_k} = \mathcal{H}([\mathbf{S}'_{\sigma\bar{x}_k} \quad \mathbf{S}'_{\sigma\delta\sigma_k}]) \quad (35)$$

where $\mathcal{H}(\cdot)$ represents a Householder transformation of the argument matrix.^{15,16}

The state and root-covariance measurement update equations are given by

$$\hat{\mathbf{x}}_k = \bar{\mathbf{x}}_k + \mathbf{K}_k (\tilde{\boldsymbol{\sigma}}_k - \bar{\boldsymbol{\sigma}}_k) \quad (36)$$

$$\hat{\mathbf{S}}_{x_k} = \mathcal{H} \left(\begin{bmatrix} \bar{\mathbf{S}}_{x_k} - \mathbf{K}_k \mathbf{S}'_{\sigma x_k} & \mathbf{K}_k \mathbf{S}'_{\sigma \delta \sigma_k} \end{bmatrix} \right) \quad (37)$$

where $\mathbf{K}_k = \bar{\mathbf{S}}_{x_k} \mathbf{S}'_{\sigma \bar{x}_k} (\mathbf{S}_{\sigma_k} \mathbf{S}_{\sigma_k}^T)^{-1}$ is the Kalman gain matrix.

Second-Order Divided Difference Filter The DD2 filter makes use of second-order divided differences to approximate nonlinear transformation of the state and covariance. The matrices of second-order divided differences are defined as

$$\mathbf{S}''_{x\hat{x}_{k_i,j}} = \frac{\sqrt{c^2-1}}{2c^2} [\phi_i(\hat{\mathbf{x}}_k + c\hat{\mathbf{s}}_{x_j}, \bar{\boldsymbol{\eta}}_k, t_k) + \phi_i(\hat{\mathbf{x}}_k - c\hat{\mathbf{s}}_{x_j}, \bar{\boldsymbol{\eta}}_k, t_k) - 2\phi_i(\hat{\mathbf{x}}_k, \bar{\boldsymbol{\eta}}_k, t_k)] \quad (38)$$

$$\mathbf{S}''_{x\eta_{k_i,j}} = \frac{\sqrt{c^2-1}}{2c^2} [\phi_i(\hat{\mathbf{x}}_k, \bar{\boldsymbol{\eta}}_k + c\mathbf{s}_{\eta_j}, t_k) + \phi_i(\hat{\mathbf{x}}_k, \bar{\boldsymbol{\eta}}_k - c\mathbf{s}_{\eta_j}, t_k) - 2\phi_i(\hat{\mathbf{x}}_k, \bar{\boldsymbol{\eta}}_k, t_k)] \quad (39)$$

$$\mathbf{S}''_{\sigma\bar{x}_{k_i,j}} = \frac{\sqrt{c^2-1}}{2c^2} [\mathbf{h}_i(\bar{\mathbf{x}}_k + c\bar{\mathbf{s}}_{x_j}, \delta\bar{\boldsymbol{\sigma}}_k, t_k) + \mathbf{h}_i(\bar{\mathbf{x}}_k - c\bar{\mathbf{s}}_{x_j}, \delta\bar{\boldsymbol{\sigma}}_k, t_k) - 2\mathbf{h}_i(\bar{\mathbf{x}}_k, \delta\bar{\boldsymbol{\sigma}}_k, t_k)] \quad (40)$$

$$\mathbf{S}''_{\sigma\delta\sigma_{k_i,j}} = \frac{\sqrt{c^2-1}}{2c^2} [\mathbf{h}_i(\bar{\mathbf{x}}_k, \delta\bar{\boldsymbol{\sigma}}_k + c\mathbf{s}_{\sigma_j}, t_k) + \mathbf{h}_i(\bar{\mathbf{x}}_k, \delta\bar{\boldsymbol{\sigma}}_k - c\mathbf{s}_{\sigma_j}, t_k) - 2\mathbf{h}_i(\bar{\mathbf{x}}_k, \delta\bar{\boldsymbol{\sigma}}_k, t_k)] \quad (41)$$

The state, state root-covariance, measurement, and measurement covariance predictions are given by

$$\begin{aligned} \bar{\mathbf{x}}_{k+1} &= \left(\frac{c^2 - n_x - n_\eta}{c^2} \right) \phi(\hat{\mathbf{x}}_k, \bar{\boldsymbol{\eta}}_k, t_k) \\ &+ \frac{1}{2c^2} \sum_{j=1}^{n_x} \left[\phi(\hat{\mathbf{x}}_k + c\hat{\mathbf{s}}_{x_{k_j}}, \bar{\boldsymbol{\eta}}_k, t_k) + \phi(\hat{\mathbf{x}}_k - c\hat{\mathbf{s}}_{x_{k_j}}, \bar{\boldsymbol{\eta}}_k, t_k) \right] \\ &+ \frac{1}{2c^2} \sum_{j=1}^{n_\eta} \left[\phi(\hat{\mathbf{x}}_k, \bar{\boldsymbol{\eta}}_k + c\mathbf{s}_{\eta_{k_j}}, t_k) + \phi(\hat{\mathbf{x}}_k, \bar{\boldsymbol{\eta}}_k - c\mathbf{s}_{\eta_{k_j}}, t_k) \right] \end{aligned} \quad (42)$$

$$\bar{\mathbf{S}}_{x_{k+1}} = \mathcal{H} \left(\begin{bmatrix} \mathbf{S}'_{x\hat{x}_k} & \mathbf{S}'_{x\eta_k} & \mathbf{S}''_{x\hat{x}_k} & \mathbf{S}''_{x\eta_k} \end{bmatrix} \right) \quad (43)$$

$$\begin{aligned} \bar{\boldsymbol{\sigma}}_k &= \left(\frac{c^2 - n_x - n_\sigma}{c^2} \right) \mathbf{h}(\bar{\mathbf{x}}_k, \delta\bar{\boldsymbol{\sigma}}_k, t_k) \\ &+ \frac{1}{2c^2} \sum_{j=1}^{n_x} \left[\mathbf{h}(\bar{\mathbf{x}}_k + c\bar{\mathbf{s}}_{x_{k_j}}, \delta\bar{\boldsymbol{\sigma}}_k, t_k) + \mathbf{h}(\bar{\mathbf{x}}_k - c\bar{\mathbf{s}}_{x_{k_j}}, \delta\bar{\boldsymbol{\sigma}}_k, t_k) \right] \\ &+ \frac{1}{2c^2} \sum_{j=1}^{n_\sigma} \left[\mathbf{h}(\bar{\mathbf{x}}_k, \delta\bar{\boldsymbol{\sigma}}_k + c\mathbf{s}_{\sigma_{k_j}}, t_k) + \mathbf{h}(\bar{\mathbf{x}}_k, \delta\bar{\boldsymbol{\sigma}}_k - c\mathbf{s}_{\sigma_{k_j}}, t_k) \right] \end{aligned} \quad (44)$$

$$\mathbf{S}_{\sigma_k} = \mathcal{H} \left(\begin{bmatrix} \mathbf{S}'_{\sigma\bar{x}_k} & \mathbf{S}'_{\sigma\delta\sigma_k} & \mathbf{S}''_{\sigma\bar{x}_k} & \mathbf{S}''_{\sigma\delta\sigma_k} \end{bmatrix} \right) \quad (45)$$

where n_x is the size of the state dimension, n_η is the size of the process noise dimension, and n_σ is the size of the measurement noise dimension.

Lastly, the state and root-covariance update equations are given by

$$\hat{\boldsymbol{x}}_k = \bar{\boldsymbol{x}}_k + \boldsymbol{K}_k (\bar{\boldsymbol{\sigma}}_k - \bar{\boldsymbol{\sigma}}_k) \quad (46)$$

$$\hat{\boldsymbol{S}}_{x_k} = \mathcal{H} \left(\left[\bar{\boldsymbol{S}}_{x_k} - \boldsymbol{K}_k \boldsymbol{S}'_{\sigma x_k} \quad \boldsymbol{K}_k \boldsymbol{S}'_{\sigma \delta \sigma_k} \quad \boldsymbol{K}_k \boldsymbol{S}''_{\sigma x_k} \quad \boldsymbol{K}_k \boldsymbol{S}''_{\sigma \delta \sigma_k} \right] \right) \quad (47)$$

where $\boldsymbol{K}_k = \bar{\boldsymbol{S}}_{x_k} \boldsymbol{S}'_{\sigma \bar{x}_k} (\boldsymbol{S}_{\sigma_k} \boldsymbol{S}_{\sigma_k}^T)^{-1}$ is the Kalman gain matrix.

Note that in the MRP pseudo-measurement model, $\boldsymbol{h}(\bar{\boldsymbol{x}}_k, \delta \bar{\boldsymbol{\sigma}}_k, t_k)$ is a linear function of the state and measurement noise. Therefore, $\boldsymbol{S}''_{\sigma \bar{x}_k, j} = \boldsymbol{S}''_{\sigma \delta \sigma_k, j} = 0$ and $\bar{\boldsymbol{\sigma}}_k = \boldsymbol{h}(\bar{\boldsymbol{x}}_k, \delta \bar{\boldsymbol{\sigma}}_k, t_k)$, which implies that the DD2 measurement update is identical to that of the DD1 filter. Due to the weakly nonlinear behavior of the MRP state dynamics, the second-order terms in the state and covariance predictions remain non-zero. For this reasons it is expected that the DD2 filter provides better performance than the DD1 filter.

Covariance Transformation Following the development in Ref. 15 and 16, a first-order divided difference transformation of the state covariance matrix to the shadow state covariance matrix suitable for the DD1 filter is given by

$$\hat{\boldsymbol{P}}_k^{S1} = \frac{1}{4c^2} \sum_{j=1}^n [\boldsymbol{\lambda}(\hat{\boldsymbol{x}}_k + c\hat{\boldsymbol{s}}_{x_j}) - \boldsymbol{\lambda}(\hat{\boldsymbol{x}}_k - c\hat{\boldsymbol{s}}_{x_j})] [\boldsymbol{\lambda}(\hat{\boldsymbol{x}}_k + c\hat{\boldsymbol{s}}_{x_j}) - \boldsymbol{\lambda}(\hat{\boldsymbol{x}}_k - c\hat{\boldsymbol{s}}_{x_j})]^T \quad (48)$$

Similarly the second-order transformation suitable for the DD2 filter is

$$\begin{aligned} \hat{\boldsymbol{P}}_k^{S2} &= \hat{\boldsymbol{P}}_k^{S1} + \frac{c^2 - 1}{4c^4} \sum_{j=1}^n [\boldsymbol{\lambda}(\hat{\boldsymbol{x}}_k + h\hat{\boldsymbol{s}}_{x_j}) + \boldsymbol{\lambda}(\hat{\boldsymbol{x}}_k - c\hat{\boldsymbol{s}}_{x_j}) - 2\boldsymbol{\lambda}(\hat{\boldsymbol{x}}_k)] \\ &\quad \cdot [\boldsymbol{\lambda}(\hat{\boldsymbol{x}}_k + c\hat{\boldsymbol{s}}_{x_j}) + \boldsymbol{\lambda}(\hat{\boldsymbol{x}}_k - h\hat{\boldsymbol{s}}_{x_j}) - 2\boldsymbol{\lambda}(\hat{\boldsymbol{x}}_k)]^T \end{aligned} \quad (49)$$

Following these covariance transformations at the switching point, the square-root decompositions of the state covariance can be calculated from Eqs. (24) and (25), which are in turn used to continue the state propagations forward in time according to Eqs. (28), (30), (38), (40), (42) and (44) until the next measurement update.

Robustness Considerations

Note that the development of the EKF, DD1, and DD2 filters in the preceding sections implicitly assume that the measurement noise distributions are Gaussian. In practice this assumption is never satisfied exactly, which can quickly degrade the filter performance and can lead to divergence in extreme cases. Techniques based on Huber's generalized maximum likelihood method have been generalized to Kalman filtering and divided-difference filtering²⁴ in order reduce the sensitivity of the filter to deviations in the assumed distributions, at a slight increase in computational burden. The same techniques can be applied here to MRP-based attitude filtering by modifying the state update equations in the EKF and DDF according to Ref. 24. Further robustness discussion is beyond the scope of this paper.

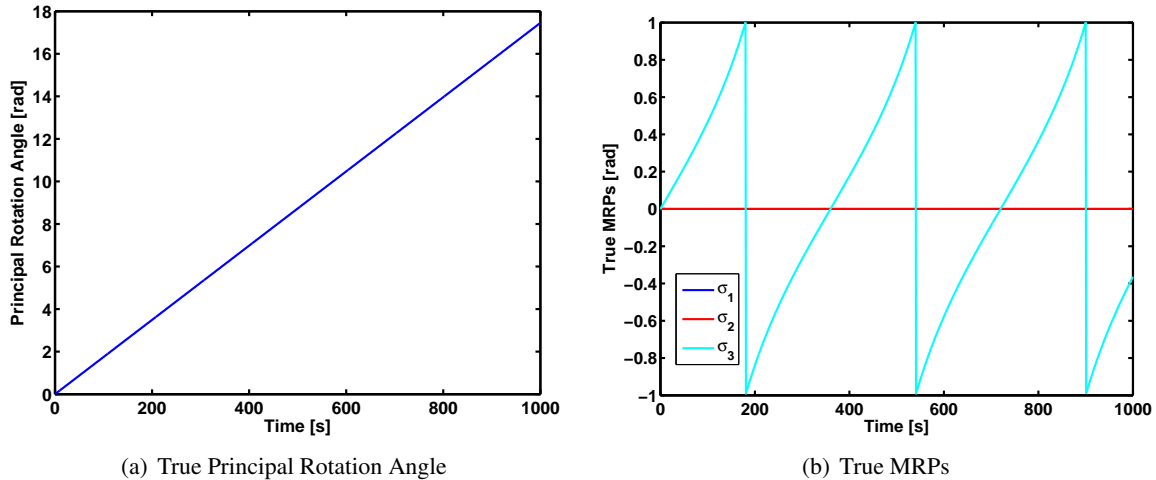


Figure 3. True Principal Rotation Angle and MRPs

EXAMPLE PROBLEM

This section describes an example problem that illustrates the MRP-based estimation techniques using the shadow set transformation for singularity avoidance. In this problem, consider a spacecraft rotating with an angular velocity of 1 deg/s about the body z-axis over a period of 1000 s. The simulation parameters are shown in Table 1. The true principal rotation angle and true MRP time history are shown in Fig. 3. Note that there are several shadow set transformations apparent in Fig. 3(b) in order to keep the MRP value within the unit sphere.

The results of a 2000 case Monte-Carlo simulation are shown Fig. 4. Figure 4(a) shows the root mean square (RMS) total attitude angle error and Fig. 4(b) shows RMS of the norm of the gyroscope bias estimate error. The Monte-Carlo simulations involve five filtering techniques: a standard Quaternion Multiplicative Extended Kalman Filter (QM-EKF),¹ a Quaternion Constrained Extended Kalman Filter (QC-EKF),⁴ an extended Kalman filter based on the MRP formulation discussed in this paper (MRP-EKF), and first and second-order divided difference filters using the MRP formulation (MRP-DD1 and MRP-DD2, respectively). In these plots, the RMS errors of the filters are shown in the solid curves while the predicted RMS error based on the filter covariance matrix are shown in the dashed curves. In this case, the QM-EKF and the MRP-EKF exhibit nearly the same overall performance. This result is not a surprise because both filters involve similar first-order approximations of the state dynamics and measurement noise. However, it can be seen in the detailed plot over the first 50 s of the simulation, Fig. 4(c) and (d), that the MRP-EKF converges faster than the QM-EKF to the steady state error level. This enhanced convergence rate is due to the fact that the MRP formulation does not require a linearization in order to enforce the quaternion norm constraint. Similarly, the QC-EKF converges to the steady state error faster than the QM-EKF over all, though its initial convergence rate is slower. The MRP-DD1 filter does not meet the same level of performance as that of the MRP-EKF case. This result is not particularly bothersome since the DD1 filter performance is usually worse than that of the EKF as seen in Refs. 15, 16 and 24. The MRP-DD2 filter exhibits the best performance overall, which is to be expected since it is a second-order filter and as a result can better capture the system nonlinearities. The uncertainty predictions based on the covariance matrix do not match the actual RMS for any of the filter results. The uncertainties can be tuned to better match the actual performance either offline or by using an

Table 1. Simulation Parameters

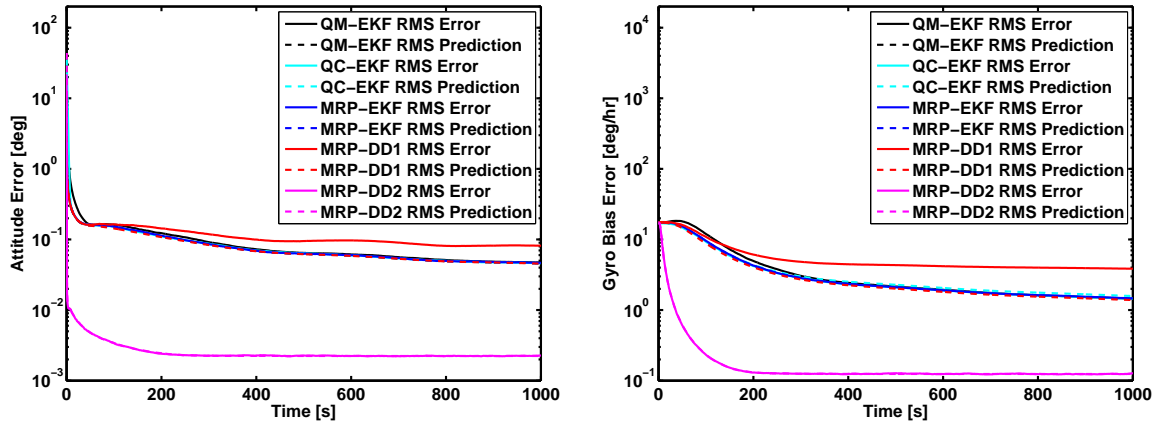
Variable	Value
Gyroscope Sample Rate	10 Hz
MRP Sample Rate	1 Hz
σ_ω^2	$10^{-13} \text{ rad}^2/\text{s}$
σ_β^2	$10^{-15} \text{ rad}^2/\text{s}^3$
σ_s^2	$7.16 \cdot 10^{-5} \text{ rad}^2$
$\hat{P}_{\sigma\sigma_0}$	$\text{diag}([0.0122 \ 0.0122 \ 0.0122]) \text{ rad}^2$
$\hat{P}_{\beta\beta_0}$	$\text{diag}([2.35 \ 2.35 \ 2.35]) \cdot 10^{-9} \text{ rad}^2/\text{s}^2$
$\hat{P}_{\sigma\beta_0}$	$\mathbf{0} \text{ rad}^2/\text{s}$
σ_0	$[0 \ 0 \ 0]^T \text{ rad}$
β_0	$[0 \ 0 \ 0]^T \text{ rad/s}$

adaptive approach to estimate the process noise covariance.²⁵

As discussed in earlier sections, the MRP switching condition can occur for any value of $\sigma_r \geq 1$. Figure 5 shows the estimator performance for values of σ_r ranging from 1 to 1000. The results are shown only for the EKF formulation of the MRP attitude filter. Clearly the estimator performance degrades as the switching surface grows in magnitude, and it can be inferred from the results that the limiting case $\sigma_r \rightarrow \infty$ leads to infinite estimation error since the MRP is reaching the neighborhood of the singularity. Similar trends occur for the DD1 and DD2 formulations. Based on these results there does not seem to be any benefit for using a MRP switching surface greater than the unit sphere but for some particular applications it may be preferable to do so. Having a general MRP covariance switching solution, however, also use to switch at any time where $\|\sigma\| > 1$. It is not required to intercept the $\|\sigma\| = 1$ surface precisely, making the numerical implementation far easier.

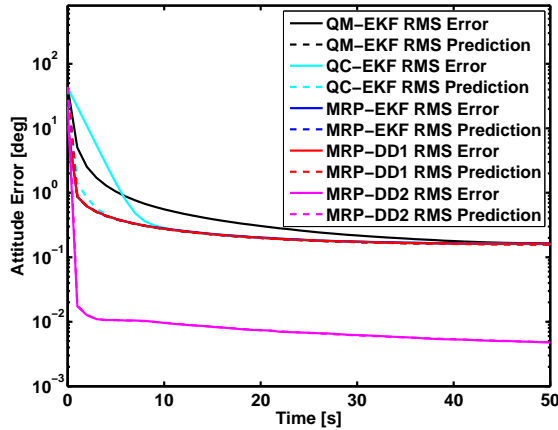
Previous applications of the MRP singularity avoidance based on the shadow set transformation have neglected the covariance mapping associated with the transformation. Fig. 6 shows a comparison of the MRP-based EKF with and without the covariance transformation to illustrate the issues associated with neglecting the transformation. At the first switching point a sharp bend can clearly be seen in the case without the covariance transformation after which the estimator performance is degraded relative to the case that includes the proper covariance transformation. This bend is due to the fact that elements of the covariance matrix must change sign during the shadow mapping since the MRP state representation changes sign during the mapping. Therefore the estimates that neglect the covariance transformation develop systematic error and are no longer optimal. The results are shown only for the EKF-based filter, similar behavior is found for the DD1 and DD2 filters.

Table 2 shows a comparison of the computational costs of each filter applied to this problem. The mean computation time is calculated for each Monte-Carlo set and then divided by the QM-EKF time to provide a relative cost comparison ratio. Also the standard deviation of the computation times are provided to show the confidence intervals. The MRP-based EKF formulation described in this paper requires slightly less computation on average than the quaternion-based EKF. These cost savings are consistent with the results of Ref. 26, which found a reduced computation using

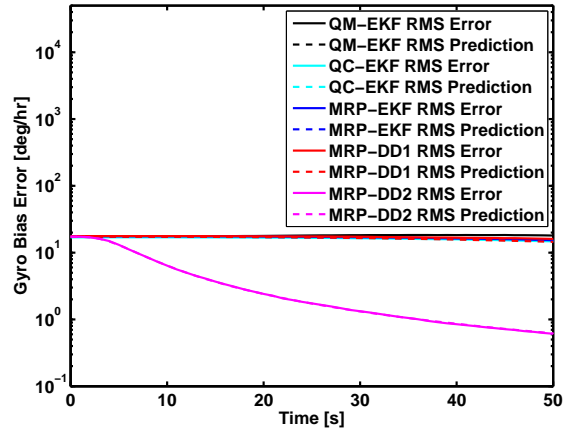


(a) Attitude Angle Estimation Error

(b) Gyroscope Bias Estimation Error



(c) Attitude Angle Estimation Error (Detail)



(d) Gyroscope Bias Estimation Error (Detail)

Figure 4. Comparison of MRP-based filters and Quaternion-based filter

the Rodrigues parameters for attitude estimation compared with the quaternion filter. The DD1 and DD2 filters require roughly the same computational cost which is consistent with Ref. 24. In this case the divided difference filters are each about an order of magnitude more expensive than the EKF.

CONCLUSIONS

This paper discusses singularity avoidance for attitude estimation based on the stereographic projection properties of the Modified Rodrigues Parameters (MRP). In this formulation, a globally nonsingular attitude representation is available using a simple switching procedure to the shadow MRP set to avoid singularities. The switching procedure includes a transformation to map the state covariance between the two representations, including gyroscope bias estimates. Covariance transformations are provided for the extended Kalman filter, as well as the first and second-order divided difference filters. An example problem illustrates the effectiveness of the singularity avoidance procedure, enabling globally non-singular attitude estimation with a minimal attitude representation. The MRP extended Kalman filter with proper state and covariance switching yields a faster ini-

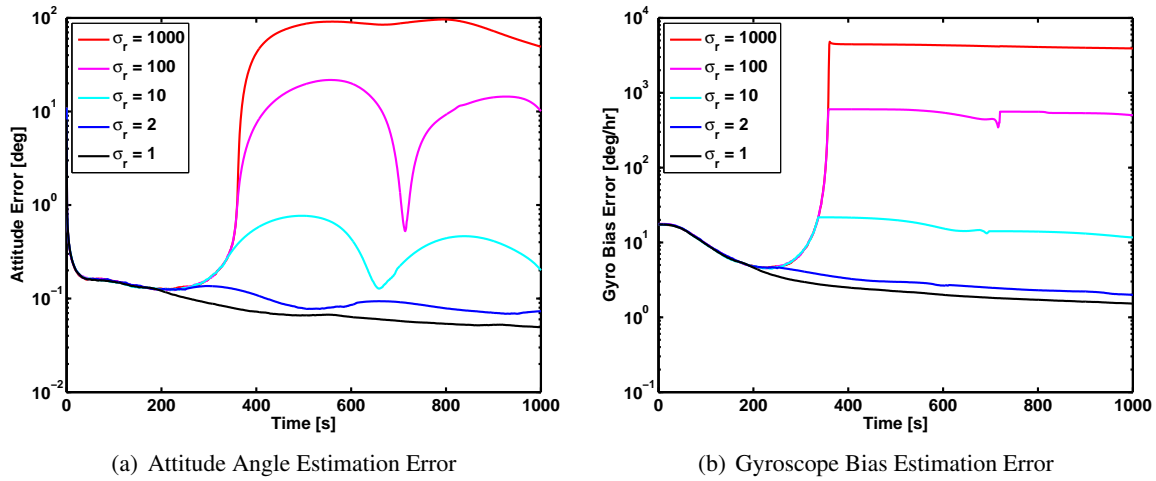


Figure 5. Comparison of MRP-based filter with varying σ_r

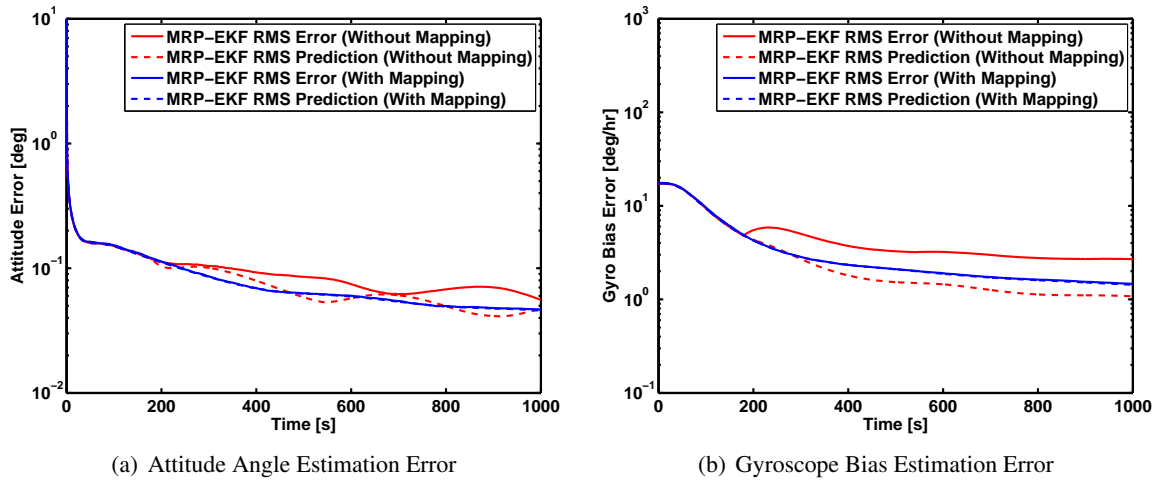


Figure 6. Comparison of MRP-based filter with and without the covariance transformation

tial convergence than the classic multiplicative or the newer constrained quaternion filter, with the computational loads being slightly reduced as well.

ACKNOWLEDGEMENT

The authors would like to thank Dr. J. Hurtado of Texas A&M for fruitful discussions on non-singular MRP attitude estimation.

REFERENCES

- [1] Lefferts, E. J., Markley, F. L., and Shuster, M. D., “Kalman Filtering for Spacecraft Attitude Estimation,” *Journal of Guidance, Control, and Dynamics*, Vol. 5, No. 5, 1982, pp. 417–429.
- [2] Crassidis, J. L., Markley, F. L., and Cheng, Y., “Survey of Nonlinear Attitude Estimation Methods,” *Journal of Guidance, Control, and Dynamics*, Vol. 30, No. 1, 2007, pp. 12–28.
- [3] Zanetti, R. and Bishop, R., “Quaternion Estimation and Norm Constrained Kalman Filtering,” American Institute of Aeronautics and Astronautics, AIAA Paper 2006–6164, August 2006.

Table 2. Computational Cost

Filter	Mean Computation Time	Standard Deviation
QM-EKF	1.000	0.015
QC-EKF	1.089	0.029
MRP-EKF	0.977	0.024
MRP-DD1	10.795	0.316
MRP-DD2	11.062	0.274

- [4] Majji, M. and Mortari, D., “Quaternion Constrained Kalman Filter,” American Astronautical Society, AAS Paper 08–215, January 2008.
- [5] Schaub, H. and Junkins, J. L., *Analytical Mechanics of Space Systems*, American Institute of Aeronautics and Astronautics, AIAA Education Series, Reston, VA, 2003.
- [6] Tsiotras, P. and Longuski, J. M., “A New Parameterization of the Attitude Kinematics,” *Journal of the Astronautical Sciences*, Vol. 43, No. 3, 1995, pp. 243–262.
- [7] Schaub, H. and Junkins, J. L., “Stereographic Orientation Parameters for Attitude Dynamics: A Generalization of the Rodrigues Parameters,” *Journal of the Astronautical Sciences*, Vol. 44, No. 1, 1996, pp. 1–19.
- [8] Schaub, H., Robinett, R. D., and Junkins, J. L., “New Penalty Functions for Optimal Control Formulation for Spacecraft Attitude Control Problems,” *Journal of Guidance, Control, and Dynamics*, Vol. 20, No. 3, 1997, pp. 428–434.
- [9] Crassidis, J. L. and Markley, F. L., “Attitude Estimation Using Modified Rodrigues Parameters,” Proceedings of the Flight Mechanics/Estimation Theory Symposium, NASA-Goddard Space Flight Center, Greenbelt, MD, May 1996, pp. 71–83.
- [10] Markley, F. L., “Attitude Error Representations for Kalman Filtering,” *Journal of Guidance, Control, and Dynamics*, Vol. 26, No. 2, 2003, pp. 311–317.
- [11] Crassidis, J. L. and Markley, F. L., “Unscented Filtering for Spacecraft Attitude Estimation,” *Journal of Guidance, Control, and Dynamics*, Vol. 26, No. 4, 2003, pp. 536–542.
- [12] Cheng, Y. and Crassidis, J. L., “Particle Filtering for Sequential Spacecraft Attitude Estimation,” American Institute of Aeronautics and Astronautics, AIAA Paper 2004–5337, August 2004.
- [13] Chen, J., Yuan, J., and Fang, Q., “Flight Vehicle Attitude Determination Using the Modified Rodrigues Parameters,” *Chinese Journal of Aeronautics*, Vol. 21, No. 5, 2008, pp. 433–440.
- [14] Lee, D. and Alfriend, K. T., “Additive Divided Difference Filtering for Attitude Estimation Using Modified Rodrigues Parameters,” American Astronautical Society, AAS Paper 08–283, June 2008.
- [15] Nørgaard, M., Poulsen, N. K. and Ravn, O., “Advances in Derivative Free State Estimation for Nonlinear Systems,” Technical University of Denmark, Department of Mathematical Modelling, Technical Report IMM-REP-1998–15, revised April 2000.
- [16] Nørgaard, M., Poulsen, N. K. and Ravn, O., “New Developments in State Estimation for Nonlinear Systems,” *Automatica*, Vol. 36, No. 11, 2000, pp. 1627–1638.
- [17] Hurtado, J. E., “Interior Parameters, Exterior Parameters, and a Cayley-like Transform,” *Journal of Guidance, Control, and Dynamics*, in review.
- [18] Tsiotras, P., Junkins, J. L., and Schaub, H., “Higher Order Cayley Transforms with Applications to Attitude Representations,” *Journal of Guidance, Control, and Dynamics*, Vol. 20, No. 3, 1997, pp. 528–536.
- [19] Farrenkopf, R. L., “Analytic Steady-State Accuracy Solutions for Two Common Spacecraft Attitude Estimators,” *Journal of Guidance and Control*, Vol. 1, No. 4, 1978, pp. 282–284.
- [20] Bruccoleri, C. and Mortari, D., “MRAD: Modified Rodrigues Vector Attitude Determination,” *Journal of the Astronautical Sciences*, Vol. 54, No. 3–4, 2006, pp. 383–390.
- [21] Crassidis, J. L. and Junkins, J. L., *Optimal Estimation of Dynamic Systems*, Chapman & Hall/CRC, Boca Raton, FL, 2004.
- [22] Van Loan, C. F., “Computing Integrals Involving the Matrix Exponential,” *IEEE Transactions on Automatic Control*, Vol. 23, No. 3, 1978, pp. 395–404.

- [23] Setoodeh, P., Khayatian, A., and Farjah, E., "Attitude Estimation By Divided Difference Filter-Based Sensor Fusion," *Journal of Navigation*, Vol. 60, No. 1, 2007, pp. 119–128.
- [24] Karlgaard, C. D. and Schaub, H., "Huber-Based Divided Difference Filtering," *Journal of Guidance, Control, and Dynamics*, Vol. 30, No. 3, 2007, pp. 885–891.
- [25] Myers, K. A. and Tapley, B. D., "Adaptive Sequential Estimation with Unknown Noise Statistics," *IEEE Transactions on Automatic Control*, Vol. 21, No. 4, 1976, pp. 520–523.
- [26] Idan, M., "Estimation of Rodrigues Parameters from Vector Observations," *IEEE Transactions on Aerospace and Electronic Systems*, Vol. 32, No. 2, 1996, pp. 578–586.